A Numerical Study of High Enthalpy Flow over a Rearward Facing Step with Rounded Corners

N.R. Deepak, S.L. Gai, and A.J. Neely

1 Introduction

The rearward facing step with a sharp corner is a classical configuration for studying separated flows. This configuration is also of practical relevance in a hypersonic vehicle. However, a truly sharp corner is basically a mathematical simplicity [9]. The influence of finite radius at the corner is therefore of significance and is studied here numerically under high enthalpy conditions using state-of-the-art computational fluid dynamics (CFD). The flow conditions are comparable to reentry velocity of 6.7 km/s which corresponds to a total specific enthalpy of $h_o \approx 26$ MJ/kg with a unit Reynolds number 1.82×10^6 per meter and a Mach number $M_\infty \approx 7.6$ with air as the test gas. The geometry consists of an upstream flat-plate of length (L) of 48.4 mm with sharp leading edge. This is followed by a step of height (h) 2 mm and then a downstream flat plate of length (D) of 109.4 mm. Three different radii, $r/h = 1/8$, $r/h = 1/3$ and $r/h = 1/1$ are considered here for the corner radius. The two-dimensional flow-field of interest is modelled using a time-dependent Multi-Block Compressible Navier-Stokes (MB-CNS) solver [6]. Perfect gas calculations were made with air to behave as a single species and real gas calculations were made assuming air to be a mixture of thermally perfect gas with 5 neutral species and adopting Gupta's kinetic scheme for chemical reactions [3]. A multi-block structured grid with 52,000 cells is used. This was arrived at after performing a grid independence study over a sharp corner and modifying the grid topology to suit the curvature for the rounded configurations. Details regarding grid convergence are given in Deepak [1].

N.R. Deepak · S.L. Gai · A.J. Neely
School of Engineering & IT, High Speed Flow Group
University of New South Wales, Australian Defence Force Academy, Canberra 2600, Australia

2 Results and Discussions

In Figure 1, Stanton number (S_t), skin friction (c_f) and pressure (p/p_∞) distributions are shown for a sharp corner for both perfect gas and real gas. Here, the top separation lip is at $s/h = 0$, $s/h = 1$ is the bottom corner of the step and $s/h \geq 1$, is the distance down the plate. The forebody data close to the top corner is shown and very near upstream of the corner, a jump is observed in both the S_t and c_f. This particular behaviour as the corner discontinuity is approached from the upstream is due to the so called Goldstein singularity [2, 8]. In this region, we note that heat flux reduces while skin friction increases for a real gas. The pressure distributions indicate a relatively constant pressure upstream of the corner and, as the corner is approached, there is a steep fall due to expansion. Of particular note is the decrease in pressure on the forebody which begins at $s/h \leq 0.25$ which is the same location at which the skin friction and heat flux start to increase. The favourable pressure gradient allows for this rise in skin friction. Over the face of the step, the Stanton number values gradually reduce and go to zero at the bottom corner and after $s/h \geq 1$ a recovery occurs in the recirculation region which continues at and after reattachment. With respect to the skin friction, it can be seen that it passes from a positive to a negative value at approximately 0.076 step heights. This is the location at which the boundary layer separates and it is not at $s/h = 0$. Downstream from the bottom corner, the skin friction reaches zero once again at s/h = 2.54 when the flow reattaches. This is 1.54 step heights from the step face. The pressure distributions indicate a continuous fall from the top corner, reaching a minimum on the face of the step at $s/h \approx 0.038$ as a result of over expansion at the corner. After $s/h \approx 0.038$, a steep recovery occurs as the flow is recompressed through a lip shock. After $s/h \approx 0.2$, a pressure plateau is seen which is consistent with the constant pressure in the recirculation region. Further increase in pressure is due to the reattachment process. The effect of real gas on S_t, c_f and p/p_∞, seem to be insignificant in the separation and reattachment regions. Based on these results, separation occurs on the face of

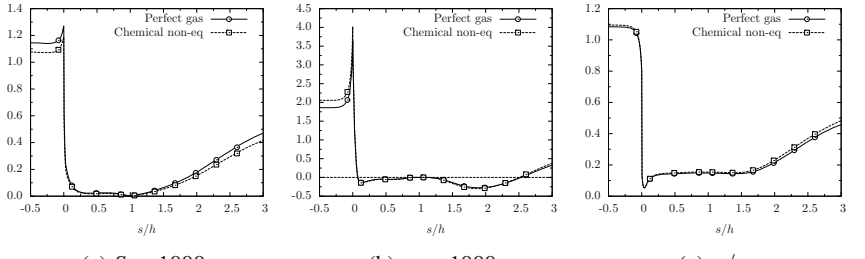

(a) $S_t \times 1000$ (b) $c_f \times 1000$ (c) p/p_∞

Fig. 1 Stanton number, skin friction & pressure distributions for sharp corner between separation and reattachment

the step ($s/h = 0.076$) and reattachment location is at $s/h = 2.54$, which is 1.54 step heights from the bottom corner. The base pressure has a value of $p/p_\infty = 0.146$.

2.1 The Near-Wake with Rounded Corners

The S_t, c_f and p/p_∞ distributions between the regions of separation and reattachment for different corner radii in comparison with those of the sharp corner were investigated. Here, the comparison is restricted to perfect gas as real gas effects were found to be insignificant in the separation/reattachment region as found earlier (Figure 1). In Figure 3, the influence of the corner radius on S_t, c_f and p/p_∞ are compared with those of the sharp corner. The coordinate system used to represent the data here is as follows. The abscissa represent the continuous wetted surface $'s'$, in which $s^* \leq 1$ refers to the normalised forebody distance, $0 \leq s/a \leq 1$, the normalised rounded corner distance and $s/h \geq 1$ the normalised distance downstream of the step. Figure 2 gives a schematic of the coordinate used to present the data. The normalisation of the forebody was obtained using the relation, $s^* = [(x - L_r)/L_r]L/h = [(x - L_r)/L_r]48.4/2$ where, x is the wetted surface coordinate running from the leading edge to the point where the forebody meets the rounded corner and L_r is the wetted distance of the upstream flat plate portion.

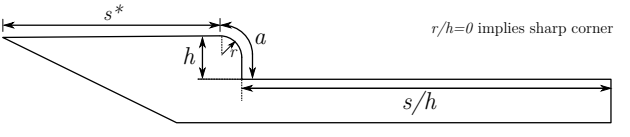

Fig. 2 Schematic representation of coordinate system for rounded corners

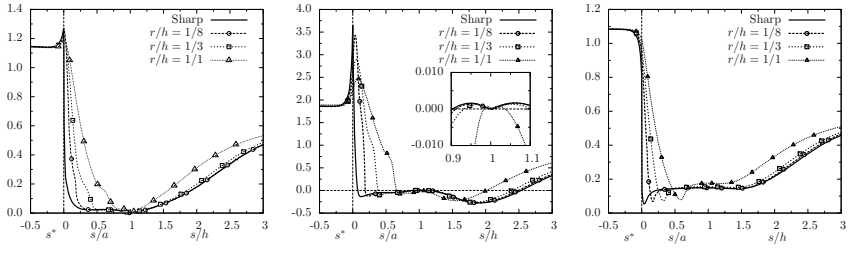

(a) $S_t \times 1000$ (b) $c_f \times 1000$ (c) p/p_∞

Fig. 3 Stanton number, skin friction and pressure distributions for different radii between separation and reattachment

Firstly, considering the heat flux in Figure 3a, over the forebody upstream of the corner, they are all nearly the same. As the corner is approached, jumps in heat flux magnitude can be seen to vary depending on the corner radius, with the maximum occurring for the sharp corner. Note that the locations of the peaks for all the rounded corners occur not exactly at $s^* = 0$ but at $s/a \approx 0.01$ which is the beginning of the curvature of the corner unlike the sharp corner, for which the peak occurs at $s^* = 0$. The Navier-Stokes solution carried out over the Mars path finder configuration [5] for various shoulder radii also showed that heat flux jumps occur at the beginning of the shoulder curvature. The effect of rounding the corner seems to be to reduce the intensity of expansion and spread it over the curved surface. The fall in heat flux is more gradual with the rounded corner and the heat flux for all the corner radii approach zero at the bottom of the step. The higher heat flux with increasing radius implies that the gas entering the recirculation region through the shear layer will be at a higher temperature for a rounded corner than for a sharp corner. Planar laser-induced fluorescence (PLIF) measurements [7] of the temperatures in the base of sharp and rounded shoulder cones showed that they were higher for the latter configuration. This lends some confidence in the higher heat flux noted for the rounded configurations. Downstream, between the bottom corner and the reattachment location ($1 \leq s/h \leq 3$), no great variations in heat flux recovery are noted, except for the fully rounded corner, for which the recovery appears to be more rapid. This is attributed to the smaller recirculation region observed for this configuration. Regarding the skin friction in Figure 3b, over the forebody region, the values are essentially the same. Similar to the heat flux, as the corner is approached, jumps in skin friction are noted and the peak values decrease with increasing radius. However, unlike the heat flux, the locations of these peaks shift slightly with increasing radius. For the fully rounded corner, the peak occurs at $s/a \approx 0.063$. It is also seen that the separation location moves further down with increasing radius. Further, the skin friction goes from negative (separation) to positive before going to zero at the bottom corner and immediately becomes positive before going negative again. These features are thought to be indicative of the presence of secondary vortices. Magnified distributions in this region are shown as inset in Figure 3b. Note that this feature is seen even for a fully rounded configuration. Figure 3c shows variation in pressure with increasing corner radius. As with skin friction, the pressure minima shift downstream with increasing radius. The pressure minima also show decreasing magnitude with increasing radius. It is also interesting to note that while the sharp corner and corner radius $r/h = 1/8$ and $r/h = 1/3$ all show a distinct and large plateau within the recirculation region, the fully rounded corner shows a much smaller plateau with higher pressures indicating a much smaller separated region. The pressure data also show that increasing the corner radius results in increased base pressure. Table 1 shows the normalised separation distances for corners of different radii. We note that the separation region has reduced by 22% from the sharp corner to a fully rounded corner and the base pressure is increased by nearly 97%. Another feature to note is that the reattachment is relatively unchanged for the sharp corner and the two smaller radii while it is substantially influenced by the fully rounded corner.

Table 1 Normalised separation and reattachment distances for the rounded corners

Configuration	Separation s/a	Reattachment s/h	Base pressure p/p_∞
$r/h = 1/8$	0.184	2.5	0.191
$r/h = 1/3$	0.374	2.4	0.220
$r/h = 1/1$	0.664	2.0	0.288

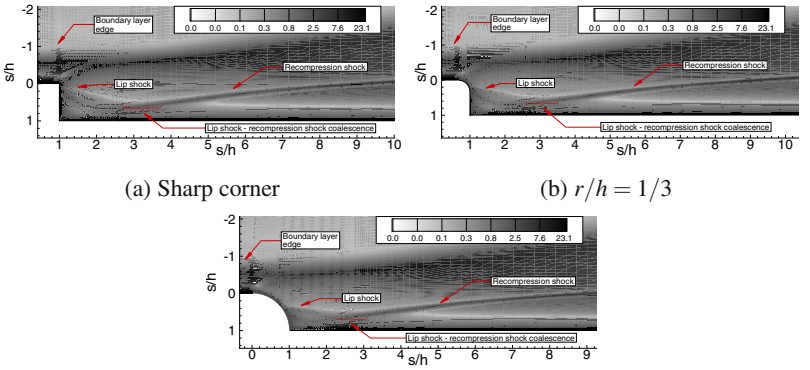

(a) Sharp corner (b) $r/h = 1/3$

(c) Rounded corner ($r/h = 1/1$)

Fig. 4 Magnitudes of density gradient ($|\nabla\rho|$) contours behind the step

In Figure 4, the magnitudes of the density gradients are shown for sharp, slightly rounded ($r/h = 1/3$) and fully rounded corner. The density gradients are calculated using $|\nabla\rho| = \sqrt{\rho_x^2 + \rho_y^2}$. Note that for the rounded corner configurations, the emergence of a weak lip shock emanating from the curved surface is clearly visible close to the location of separation. Further, the lip shock seems to be embedded within the shear layer and seems to coalesce with the recompression shock at about 3 step heights. Compared to that of the sharp corner, the lip shock inclination becomes nearly parallel to the bottom plate as the corner radius increases. This feature of lip shock orientation has been confirmed by previous researchers [4, 7]. It is also seen that with increase in radius, the confluence of lip shock and recompression shock moves closer towards the base.

3 Conclusions

A numerical study of the flow behind a rearward facing step with sharp and rounded corners in a high enthalpy hypersonic flow has been carried out. It was found that in the separated and reattachment region, the real gas effects were not significant.

For the rounded corners, flow separation was seen to occur over the curved surface and it progressed downstream with increase in the corner radius. This is consistent with previous high supersonic and hypersonic Mach number experiments [4, 7]. With increased radius, the strength of expansion decreased and, the pressure minima occurred further down the curved surface. The pressure remained nearly constant within the recirculation region, except for the fully rounded corner where the plateau region was hardly noticeable and the base pressure was much higher. Between the bottom corner and the location of reattachment, heat flux variations among different radii were not significant except for the fully rounded corner. Also, for a fully rounded corner, a much higher heat flux in the separation region was noted. A detailed visualisation of the lip shock structure was made for the rounded corners. The lip shock was seen for all the rounded configurations. The orientation of the lip shock gradually changed with increase in the corner radius and tended to become nearly parallel to the plate for the fully rounded corner. The confluence of the lip shock and the recompression shock was also seen to move closer to the base with increase in corner radius.

References

[1] Deepak, N.R.: Computational Studies of Hypersonic High Enthalpy Separated Flows. PhD thesis, School of Engineering & IT, University of New South Wales, Canberra, Australia (Submitted November 2010)
[2] Goldstein, S.: On laminar boundary-layer flow near a position of separation. Quart. J. Mech. Applied Math. 1, 43–69 (1948)
[3] Gupta, R.N., Yos, J.M., Thompson, R.A., Lee, K.-P.: A review of reaction rates and thermodynamic and transport properties for an 11-species air model for chemical and thermal nonequilibrium calculations to 30 000 k, Technical Report 1232, NASA (1990)
[4] Hama, F.R.: Experimental studies on the lip shock. AIAA Journal 6(2), 212–219 (1968)
[5] Hollis, B.R.: Experimental and Computational Aerothermodynamics of a Mars Entry Vehicle. PhD thesis, Aerospace Engineering, North Carolina State University, Raleigh, North Carolina, USA (1996)
[6] Jacobs, P.A.: Mb-cns: a computer program for the simulation of transient compressible flows. Technical Report 7/98, Department of Mechanical Engineering, University of Queensland, Brisbane (1998)
[7] O' Byrne, S.: Hypersonic Laminar Boundary Layers and Near-Wake Flows. PhD thesis, The Australian National University, Canberra (2002)
[8] Stewartson, K.: On the flow near the trailing edge of a flat plate. Proc. Roy. Soc. A. 306(1486), 275–290 (1968)
[9] Weinbaum, S.: On the singular points in the laminar two-dimensional near wake flow field. Journal of Fluid Mechanics 33(1), 39–63 (1968)